Non-destructive three-dimensional evaluation of biocompatible materials by microtomography using synchrotron radiation

Bert Müller[*ab], Philipp Thurner[c], Felix Beckmann[d], Timm Weitkamp[e], Christoph Rau[e], Ricardo Bernhardt[f], Erdal Karamuk[a], Ludwig Eckert[a], Jörg Brandt[g], Stefan Buchloh[a], Erich Wintermantel[a], Dieter Scharnweber[f], Hartmut Worch[f]

[a]Biocompatible Materials Science and Engineering, ETH Zürich, CH-8952 Schlieren
[b]Computer Vision Laboratory, ETH Zürich, CH-8092 Zürich, Switzerland
[c]Federal Laboratories for Materials Testing and Research, CH-8900 Dübendorf, Switzerland
[d]Hamburger Synchrotronstrahlungslabor HASYLAB at Deutsches Elektronen-Synchrotron DESY, D-22607 Hamburg, Germany
[e]European Synchrotron Radiation Facility, F-38043 Grenoble, France
[f]Institute of Materials Science, Dresden University of Technology, D-01062 Dresden, Germany
[g]Experimentelle Orthopädie, Martin-Luther-Universität Halle-Wittenberg, D-06112 Halle, Germany

ABSTRACT

Microtomography based on synchrotron radiation sources is a unique technique for the 3D characterization of different materials with a spatial resolution down to about 1 µm. The interface between implant materials (metals, ceramics and polymers) and biological matter is non-destructively accessible, i.e. without preparation artifacts. Since the materials exhibit different X-ray absorption, it can become impossible to visualize implant material and tissue, simultaneously. Here, we show that coating of polymer implants, which are invisible in bone tissue, does not only improve the interfacial properties but also allow the imaging of the interface in detail. Titanium implants, on the other hand, absorb the X-rays stronger than bone tissue. The difference, however, is small enough to quantify the bone formation near interface. Another advantage of microtomography with respect to classical histology is the capability to examine samples in a hydrated state. We demonstrate that ceramic hollow spheres can be imaged before sintering and fibroblasts marked by OsO_4 are visible on polymer textiles. Consequently, scaffolds of different materials designed for tissue engineering and implant coatings can be optimized on the basis of the tomograms.

Keywords: Microtomography, synchrotron radiation, biocompatible materials, implants, fibroblasts

1. INTRODUCTION

Biocompatibility is defined as the property of a material that characterizes the integration of the medical implant into the desired biological environment. This definition does not allow the quantification. This applies also to other definitions presently used for biocompatibility, since it is a very complicated materials property as it depends on many impact factors and on the specific environment. Nevertheless, we know that surface composition and topography as well as mechanical properties and stimuli can modify the biocompatibility of an implant. This knowledge gives us the possibility to tailor the biocompatibility in a more or less arbitrary manner. The verification of improvements, however, requires a suitable 3D imaging technique, which monitors the implant performance stepwise in time. This implies that the technique has to be preferably non-destructive. In order to obtain sufficient contrast in tomography, one has to choose a probe with an appropriate cross section. Both, electrons and visible light, often used for the visualization in biology, are useless for the 3D characterization of opaque implants. X-rays, on the other hand, are well suited for samples of millimeter size. Because the interactions between X-rays and matter decrease with increasing energy, the

[*]bmueller@vision.ee.ethz.ch; phone ++41 1 6336190; fax ++41 1 6321199; www.vision.ee.ethz.ch
felix.beckmann@desy.de; phone ++49 40 8998 4535; fax ++49 40 8998 2787

contrast can be adjusted to the sample geometry minimizing the measuring time. Consequently, synchrotron radiation-based microtomography[1,2] is the method of choice to make visible medical implants. However, there are some restrictions in the simultaneous visualization of implant and tissue using the attenuation contrast mode. If the attenuation of the X-rays within implant and tissue differs drastically, the low absorbing component can become invisible. Hence, the quality of the interface between implant and tissue, which determines the implant performance, becomes inaccessible. The present paper attends these limits for typical implant materials. On the other hand, we demonstrate the power of synchrotron radiation-based microtomography in the qualitative and quantitative 3D analysis of all classes of biocompatible materials presently in use, i.e. metals, ceramics and polymers.

2. THE SPATIAL RESOLUTION AND THE COMPARABILITY OF X-RAY MICROTOMOGRAPHY

There are a number of definitions that characterize the spatial resolution in tomograms. Different manufacturers use definitions, which help them to sell their system. Even if identical definitions used, the measured spatial resolution depends on the sample itself. Therefore, the comparability is restricted to the sample chosen. From a physical point of view, however, one should always verify how the spatial resolution of the individual experiment has been determined. The quality of the tomographical reconstruction can be characterized by the highest spatial frequency resolvable in the tomogram. The modulation transfer function (MTF) is a measurable and objective value characteristic for the whole system. However, there exist different methods to calculate the MTF from the measured projections. For example, by the use of sinusoidal patterns, one can directly determine the MTF of one spatial frequency measuring the minima and maxima in the projection. Another, more sophisticated approach is based on a variable slit. By calculating the Fourier transform of the measured and the theoretical projection the MTF values for several spatial frequencies can be obtained simultaneously. A continuous MTF can be found from an edge function.[3,4] Therefore, at HASYLAB we prefer the latter approach described in more detail.

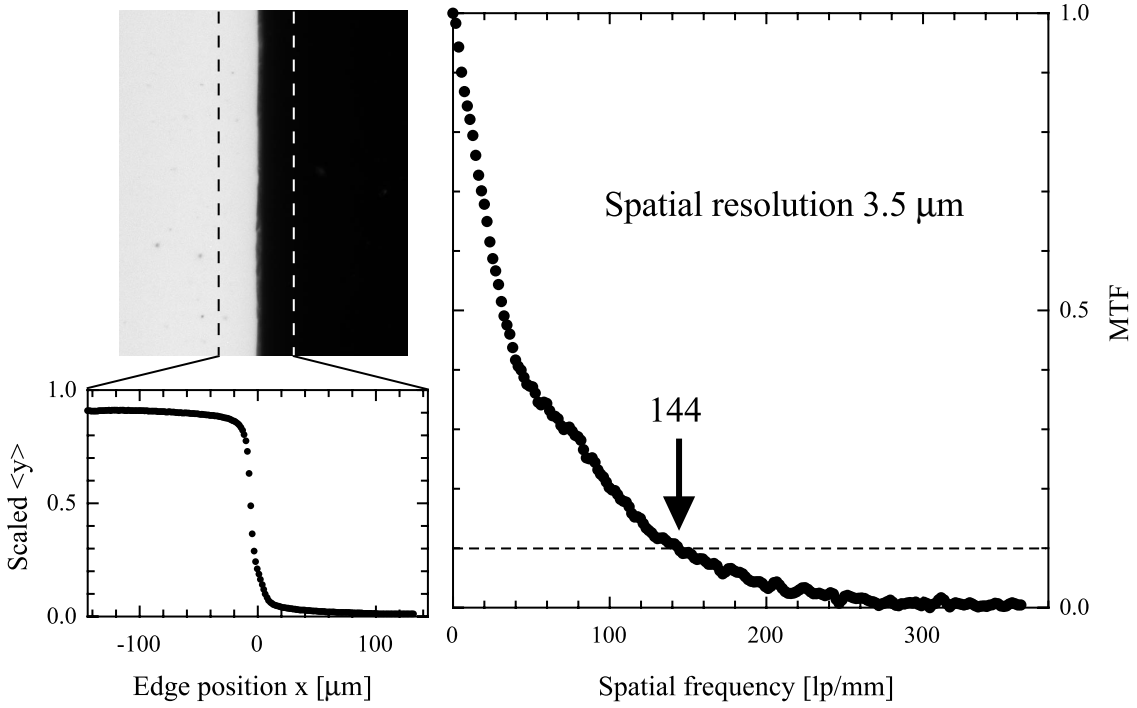

Figure 1: Determination of the spatial resolution at HASYLAB. A projection of an edge of a gold plate is recorded, as shown in the upper part on the left. Then the line scans are integrated and normalized along the edge to obtain the edge function, lower part on the left. Subsequently, the MTF is experimentally determined, whereby the spatial resolution is defined to be the crossing point of MTF at 10 percent of contrast.

The projection of an edge of a gold foil is recorded. Subsequently, the data are integrated along the edge to obtain the edge function. The projection (measured data), the related edge function and MTF are shown in Figure 1. The spatial resolution of the system, which corresponds to the half of the spatial frequency, is defined to be the value, where the spatial frequency reaches 10 percent of the MTF. For the present measurement of a porous titania ceramic, shown in Figure 2, we have found for the spatial frequency 144 linepairs per mm that finally results in a spatial resolution of 3.5 µm. It should be finally noted, that the spatial resolution is only reachable under optimal conditions. The specifics of the sample can make the spatial resolution worse.

3. MICROPOROUS TITANIA CELL CARRIERS OF SPHERICAL SHAPE WITH A CENTRAL OPENING

Titania belongs to the promising ceramic biomaterials known to be highly biocompatible. It has been successfully established for implants and cell carriers. The biocompatibility, however, also strongly depends on the 3D shape both on microscopic and macroscopic scale and the desired biological environment. As experimentally proven for alumina,[5] the macroscopic hollow sphere with a central opening can induce tissue in-growth and vascularization. The microporosity allows furthermore the supply of the cells inside the spheres with oxygen and other nutrients. The optimization of the shape for the desired medical application requires a defined fabrication process well before any clinical application. The potential improvement of the hollow sphere fabrication has to be verified. Here, a major input usually comes from the imaging techniques. Surface sensitive techniques give only limited information because it is extremely difficult to have a look inside the spheres and even impossible to characterize the inner structure - including the micro-porosity - of the walls.

Titania hollow spheres, 100 to 500 µm in diameter, with a central opening are produced by spray drying and subsequent sintering at temperatures higher than 1000 °C. The image in the upper part on the left in Figure 2 shows that the hollow spheres glued onto a glass capillary are inhomogeneous with respect to size and shape. Due to the kind of fixation the smaller spheres occur much more frequently on a glass capillary then larger ones. Some of the hollow spheres, however, are thought to have already the appropriate shape and porosity, as can be seen by the other images of Figure 2, which represent one sphere with higher magnification. A virtual cut, shown in the lower part permits a detailed study of the macroscopic inner shape of the hollow sphere. Although the microporosity is accessible by the integral absorption and even visible, the individual crystallites are not yet visible as a result of the limited resolution of tomography at HASYLAB (BW 2). The crystallites can be made visible at ESRF taking advantage of the edge enhancement of coherent synchrotron radiation sources of the third generation.[6] The quantification of crystallite sizes, however, is still questionable.

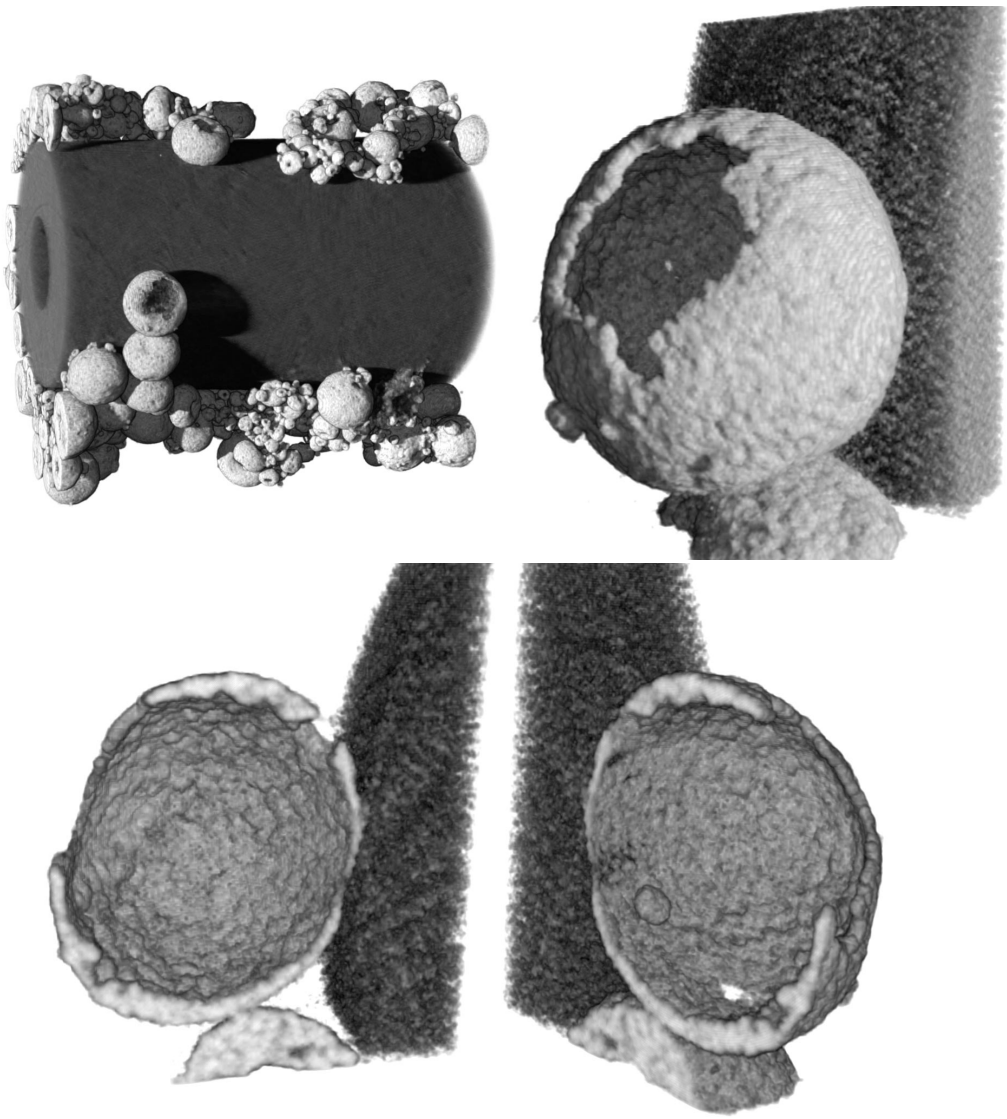

Figure 2: Spray dried titania hollow spheres. The sphere in the center with a mean diameter of 180 µm is represented with higher magnification. Tomographical scans have been performed at the beamline BW 2 at HASYLAB using a photon energy of 19 keV. As shown in Figure 1, the spatial resolution corresponds to 3.5 µm. The tomogram reveals the macroscopic shape of the spheres and their porosity.

Another fabrication technique is applied to produce larger titania hollow spheres having diameters between 500 and 3000 µm. The spheres, also with a central opening, are produced by a patented dip coating process.[7,8] Here, the ceramic slurry is a water-based titania natrium alginat suspension, which forms a gel after the exchange of Na^{+} ions by two-valent ions such as Ca^{2+}. The green bodies, which already have the macroscopic shape of the cell carriers, still contain a high amount of water. Therefore, the variety of methods to study the micro- and macrostructure is limited. Synchrotron-radiation-based microtomography, however, is not restricted to vacuum conditions. Consequently, microtomography can be used to compare the structure of the green bodies with that of the sintered hollow spheres even in a quantitative manner. An important question to optimize the fabrication is for example the shrinking of the spheres during the sintering process. Although the visualization of the ceramics is established, software tools to quantify the shape and porosity have to be developed.

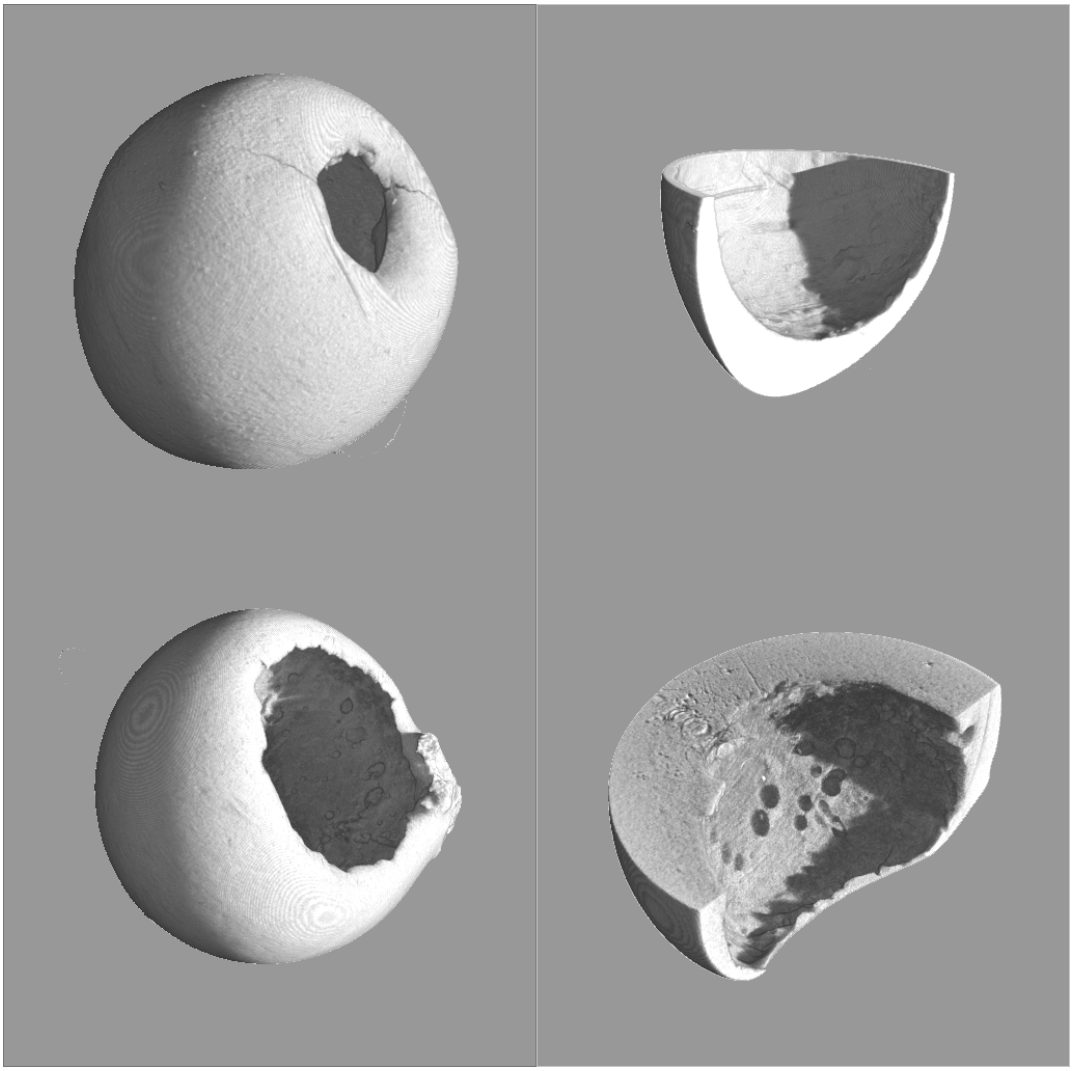

Figure 3: 3D representation of hollow spheres with a diameter of about 2000 µm before (top) and after (bottom) sintering. The measurements have been performed at the beamline BW 2 at HASYLAB using the photon energy of 24 keV. The spatial resolution corresponds to 4.5 µm.

4. POLYMER SCAFFOLDS

Porous structures can be generated out of filaments, which can be quite complex, as we know from textiles. Textiles have also many medical applications. Here is a great empirical knowledge. However, the relationship between porosity and clinical success is rather obscure since the quantification of the porosity on the different length scales is difficult to obtain. In this context, microtomography should be very helpful especially for complex 3D textiles. A prominent example is given in Figure 4, where a polyamide monofilament is combined with a polyester multi-filament.[9] The photon energy can be chosen such that the contour of the textile is easily extractable. That means the porosity can be quantified. Furthermore, one can discriminate between polyamide and polyester due to the different absorption. Consequently, a medical textile can be visualized by synchrotron radiation-based microtomography, a prerequisite to study the interface between a polymer material and the biosystem. This example demonstrates that a 3D method is necessary to examine the tissue in-growth into complex scaffolds.

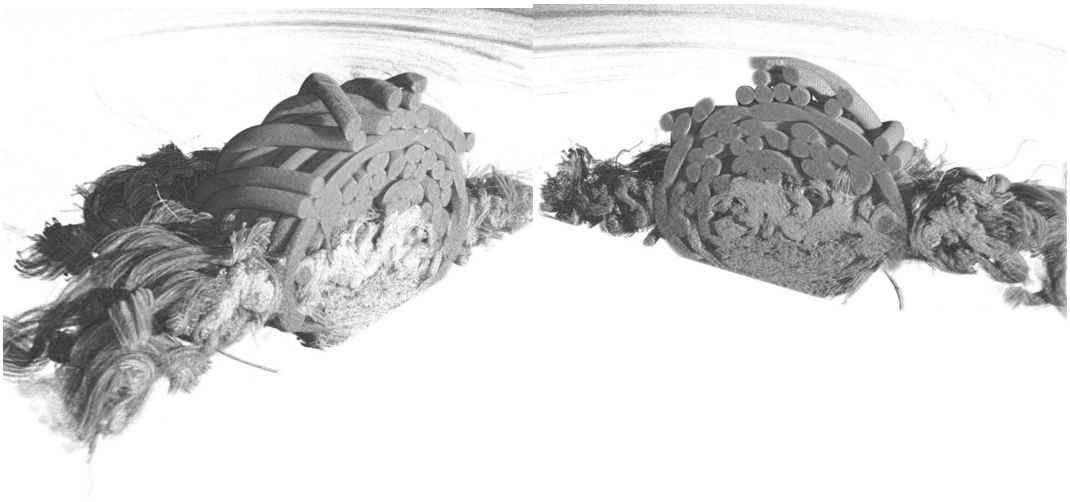

Figure 4: Complex porous textile structure consisting of a polyamide mono-filament yarn with a diameter of 110 µm and a multi-filament polyester yarn with 24 filaments each with a diameter of 20 µm. The measurements have been performed at the beamline BW 2 at HASYLAB using the photon energy of 24 keV. The spatial resolution corresponds to 4.5 µm.

An important step to characterize the tissue in-growth is the simultaneous visualization of polymeric textile and cell cultures. Here, the final aim is the determination of the locations of individual biological cells in 3D. To be comparable to well established electron microscopy, we have represented a dried sample as prepared for the characterization by electrons under vacuum conditions (Figure 5, top). Already in the projection, one can see the remains of the dried cell culture on the scaffold and distinguish between them. The interfaces, especially between polymer filaments and air, are well reproduced as a result of the edge enhancement at the synchrotron radiation source in Grenoble. The quantification of the tomogram, however, would not represent the full information on the *in vitro* cell culture because of preparation artifacts during the drying process. Therefore, it is highly desirable to characterize the cell culture including the polymer scaffold under hydrated conditions, as close as possible to the physiological conditions.

Since biological cells contain mainly water, the difference in absorption between water or phosphate buffered saline (PBS) or hydrogel, on one hand, and the cells, on the other hand, is too small to make the cells visible. Even the in-line phase contrast at ESRF does not provide any visible structure, although at typical photon energies of about 20 keV the effect is said to be orders of magnitudes higher. In order to master this problem, one can stain the cells by heavy elements such as gold or osmium. Our sample, which consists of rat tendon fibroblasts seeded on textured poly-ethylene-teraphtalate (PET) multifilament yarn, is held in a low absorbing glass capillary.[10] It is embedded in a hydrogel matrix. As discussed, the fibroblasts are as low in X-ray absorption as the surrounding embedding material. Consequently, they have to be stained with a higher absorbing contrast agent. Here, OsO_4 was used, similar to sample preparation for scanning electron microscopy, interrupted just before drying of the samples: The rat tendon fibroblasts were fixated in 3% glutaraldehyde in PBS overnight. After washing them once they were transferred into a bath with 0.1% OsO_4 for 1 h. After this procedure, the samples were washed twice with PBS and then put into the glass capillaries about 10 µm thick. The diameter of the capillaries was selected to be 0.7 mm in order to use the optics at beamline ID 22 for highest resolution.[11] The samples were embedded into a fibrin hydrogel to avoid dehydration during the measurement. 1250 projections of each sample were taken at 20 keV photon energy. The obtained spatial resolution was estimated to be 1.3 µm (voxel size 0.66 µm). As shown in Figure 5 bottom, the cells, marked by OsO_4, become a relatively strong absorber. This staining results in tomograms, where one can clearly see the cells but not discriminate between individual cells. Even these tomograms are meaningful, since we are able to uncover the location of the cells at the periphery of the thread, a proposition, which cannot be made by a 2D technique without cutting the sample. Still the concentration of staining material has to be adapted. It is too high for the sample shown in Figure 5.

In conclusion, although important steps are made in the characterization of cell cultures on polymer scaffolds in a hydrated state, the staining of the fibroblasts has to be improved.[10]

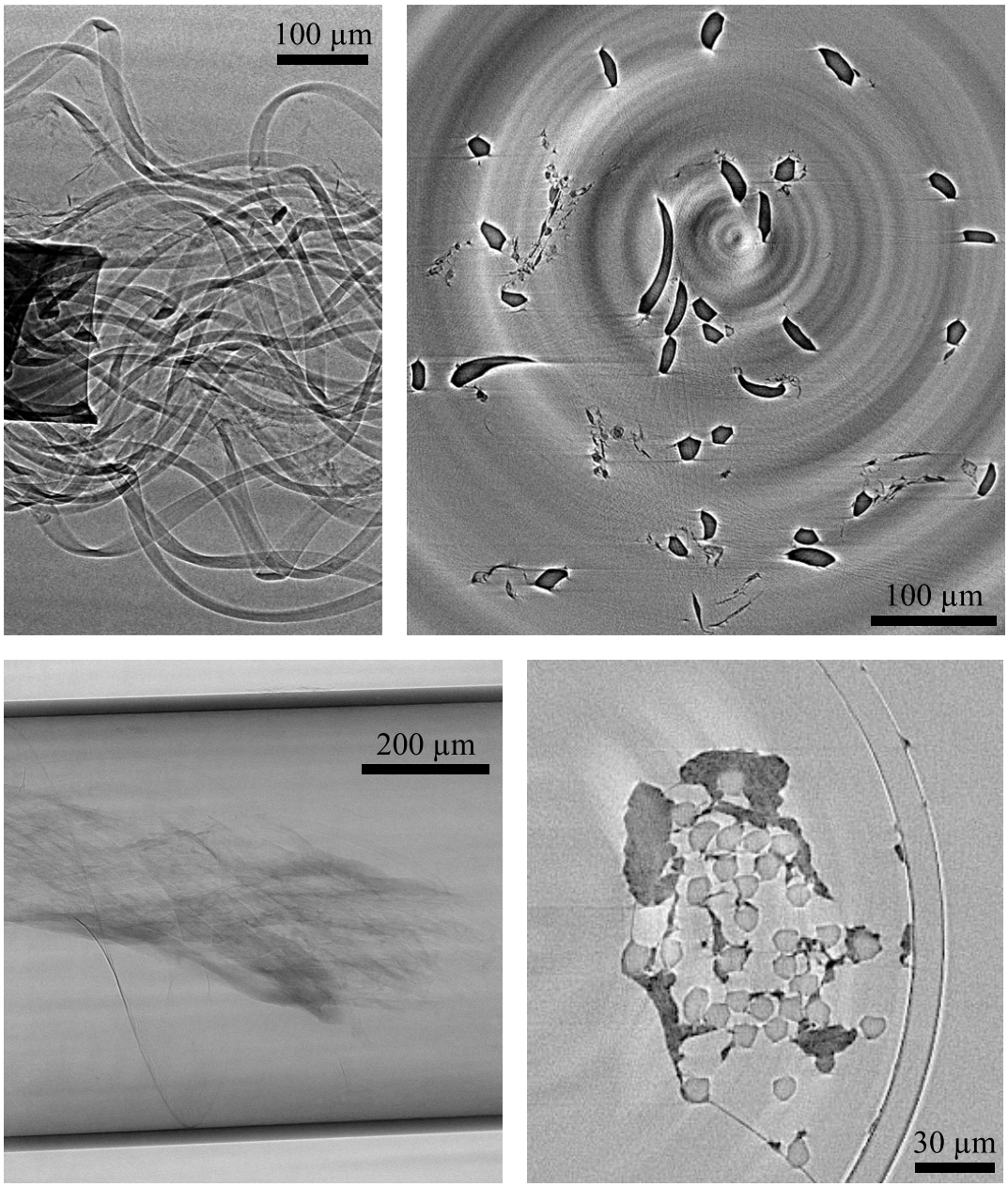

Figure 5: Fibroblasts on textured PET thread consisting of 24 filaments each 20 µm in diameter. Projection and reconstructed slice of the critical point dried sample (top) and in the hydrated environment (bottom). The measurements have been performed at the beamline ID 22 at ESRF using the photon energy of 17 keV (top) and 20 keV (bottom), respectively.

5. STRUCTURAL HISTOLOGY OF BONE EXPLANTS

The appropriate choice of materials including their structure for the construction of implants is crucial regarding long term stability, function, and compatibility. The implant can be optimized in an iterative manner: First the production

process is modified. Second, the subsequent 3D characterization of the interface between implant and the adjacent bony tissue after biopsy motivates further modifications. The structural characterization is usually done by optical or electron microscopy after the specimen is cut into thin slices of about 50 µm. This method is destructive and often results in preparation artifacts. These artifacts are crucial especially for fiber reinforced polymer implants, because cutting and polishing processes can transport particle of micrometer size into the adjacent tissue. The clinically important question of particle release cannot be answered any more. Therefore, microtomography, a nondestructive technique, provides complementary information to conventional histology.

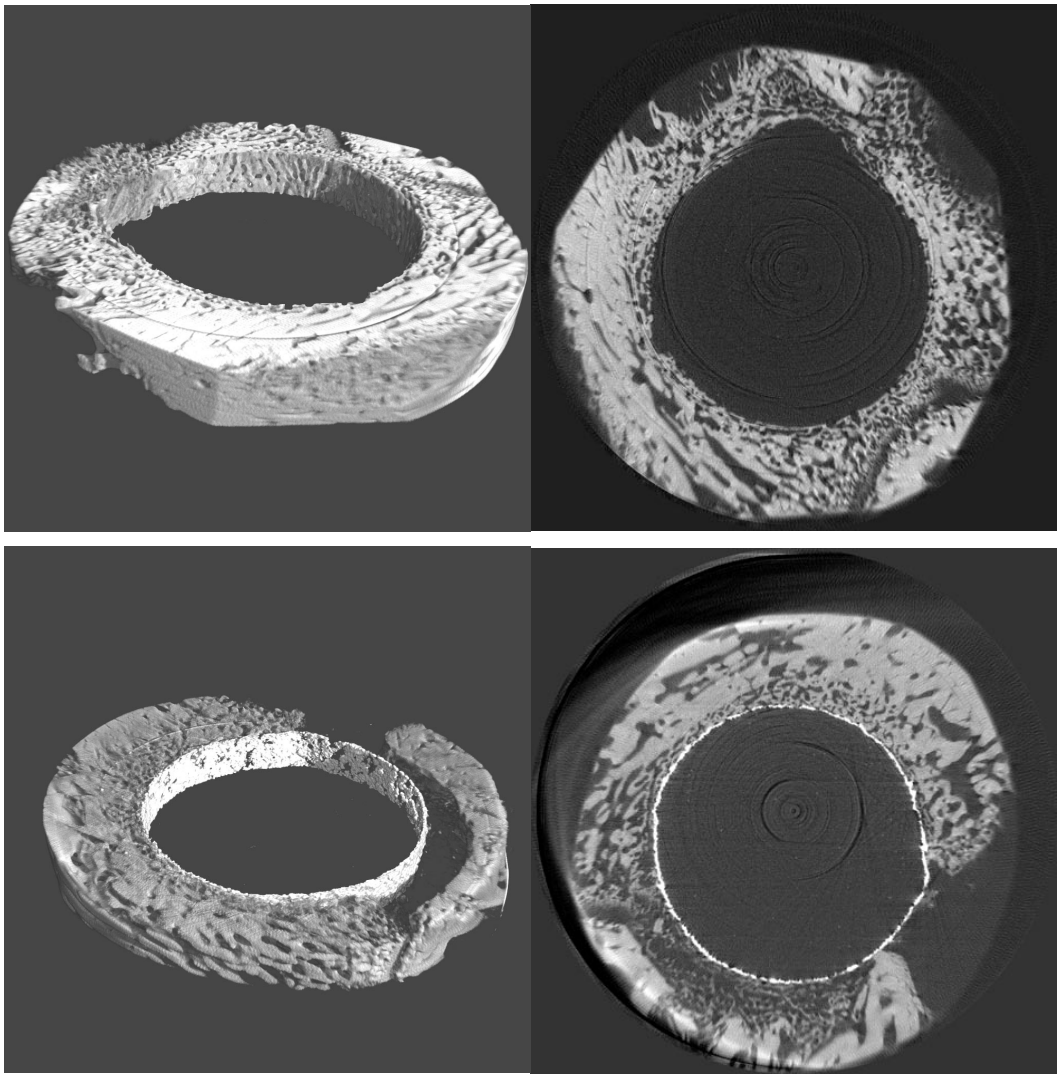

Figure 6: 3D representation and a typical slice (9.3 mm x 9.3 mm) of a tomogram obtained from a polymer explant (invisible) and the surrounding bone tissue. The data are recorded with a spatial resolution of 9.3 µm at the beamline BW 2 using a photon energy of 24 keV. PEEK explants 5 mm in diameter without coating (top) and with Ti and hydroxyapatite coating (bottom). The images of the coated explant reveal the close contact between implant and bone.

Rods of carbon fiber reinforced polyetheretherkethone (PEEK) were implanted into the femural rabbit condyle.[12] After 2 weeks, they are removed and embedded into epoxy resin for the histology. In order to improve the interface between implant and bone, half of the implants were coated by titanium and hydroxyapatite each 50 µm thick. Figure 6 shows

that the bare implants are invisible at a photon energy of 24 keV, typically used to visualize bone, due to their very low absorption. Therefore, it is impossible to determine the quality of the interface from this tomogram. If the implants are coated by a material, which has an absorption similar, but not identical, to that of the adjacent bony tissue, fulfilled for hydroxyapatite/titanium, the interface becomes detectable. The result, also shown in Figure 6, illustrates that the potential gap between implant and bone is smaller than the spatial resolution. Therefore, we conclude, the interface formed between implant and bony tissue is of good quality, since the potential fibrous encapsulation is well below 10 µm. The result is corroborated by classical histological images.[6,12]

Another method to visualize polymer implant materials is to add a higher absorbing component such as hydroxyapatite to the polymer matrix. Such a component can be homogeneously distributed or not. Inhomogeneously distributed hydroxyapatite in a hydroxyethylenemethacrylate-lactide copolymer is shown in Figure 7. This promising composite is developed to be used as bone cement. This bone cement is partially resorbable and, therefore, designed for a limited time of function in the body. Implemented into a rabbit condyle it should guide the bone in-growth into pores formed during degradation. Besides shrinking holes, the preliminary study shows that at the time of investigation the bone contact is restricted to a few dot-shaped points. The trabeculae do not form larger volumes to dock at the implant surface. Microtomography thus provides 3D images, which uncover the integration of the polymer into bone. This bone tissue-implant interface has to be adopted to improve the mechanical loadability.[13]

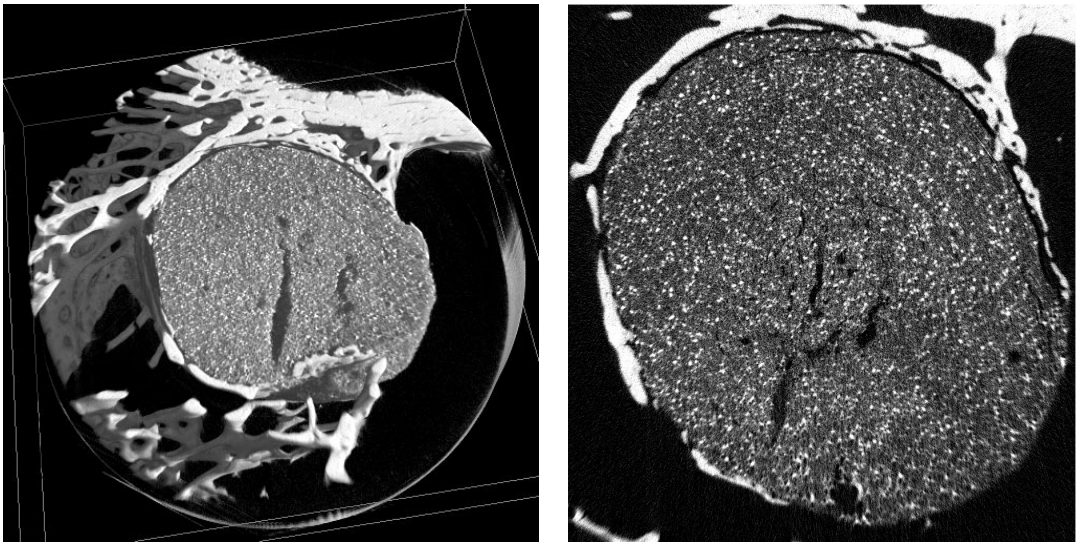

Figure 7: 3D representation and a typical slice (9.3 mm x 9.3 mm) of a tomogram obtained from bone cement and the surrounding bone tissue. The data are recorded with a spatial resolution of 9.3 µm at the beamline BW 2 using the photon energy of 24 keV. PEEK explants 5 mm in diameter without coating (top) and with Ti and hydroxyapatite coating (bottom). The images of the coated explant reveal the close contact between implant and bone.

Generally, metals are better suited than polymers for loaded implants because of their superior mechanical properties. Titanium is highly biocompatible.[14] Of course, it is not the titanium itself but its oxide formed. Therefore, the biocompatible properties can be further improved by modification of the native oxide or other coatings. The only problem is the verification of the improvement. Here, microtomography can provide essential contributions.

The osteoconductivity of Ti6Al4V explants differently bio-functionalized before implantation is quantitatively treated using a special geometry for implantation. In an animal experiment, implants of cuboid shape were placed into cylindrical holes in the jaw of dogs.[15] The explants were removed after one month together with the surrounding tissue and embedded into PMMA. The tomograms are obtained at beamlines BW 5 (HASYLAB at DESY) using a photon energy of 60 keV. The spatial resolution was found to be 9.5 µm.

In order to quantify the amount of bone formed near the titanium implants as a function of surface modification, an image-processing algorithm based on the scientific software package AVS/Express® has been developed.[16,17] The bony tissue, the embedding material and titanium implant are separated according to their different absorption behavior. For each tomogram the bone/titanium interface was determined. From this interface the contour was increased voxelwise. Hence, the relative amount of bone is uncovered as a function of distance from the interface.

Figure 8 shows a 3D representation of the explant. With respect to conventional microfocus X-ray sources, the artifacts at the interface between the cuboid titanium implant and the bone are minim. The slice, also shown in Figure 8 reveals that the bone near implant can be visualized although the titanium exhibits much stronger absorption. In order to get a quantitative idea of the bone formed, the slices can be integrated along the symmetry axis, as shown on the right in Figure 8. These quantitative data can be compared for different surface modifications, as we will show in a forthcoming paper.[18]

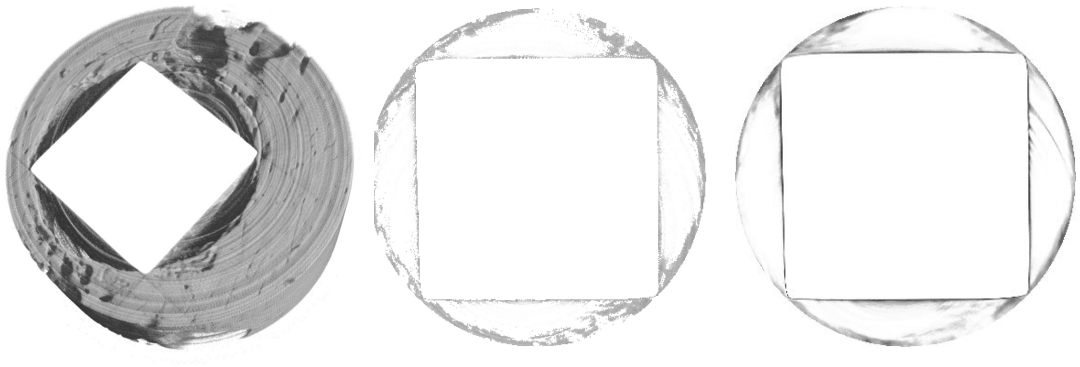

Figure 8: Titanium explants with bone tissue: 3D-representation (left), a typical slice showing only the bone formed after one month – the implant and the surrounding bone are made transparent (center), integration of about 1000 slices, revealing the bone formation along the implant (right). The cross section of the titanium implant corresponds to about 3.5 mm x 3.5 mm. The measurement was performed at BW 5 (HASYLAB at DESY) using a photon energy of 60 keV. The spatial resolution corresponds to 9.5 µm.

6. CONCLUSION

Microtomography using synchrotron radiation is the 3D imaging technique that allows the visualization of a great variety of materials. The macroscopic shape and the microscopic structure of all kinds of biomaterials, i.e. metals, ceramics and polymers, can be uncovered. With respect to electron based techniques, which require dried or frozen samples, X-ray microtomography tolerates investigations of hydrated samples even close to physiological conditions. Therefore, the interface between the material and the adjacent tissue is accessible without destruction of the sample. Thus, potential preparation artifacts are avoided, and dynamic processes such as cell migration and crack formation can be tracked in principle. It should be further noted that the retrieved data are fully quantitative *per se*, in contrast to many other imaging techniques.

The huge data sets of GB size require the development or at least adaptation of image processing algorithms to extract meaningful parameters out of the tomograms. First essential steps are made. The automated analysis, however, that would, e.g. in the case of explants easily provide the complementary results to classical histology is not yet available. Such algorithm are under development and still available for special geometries.[18]

ACKNOWLEDGEMENTS

The financial support of the Swiss National Science Foundation (contract 2153-057127.99) and of the German National Science Foundation (contract WI 1897/1-1 and WO 494/10-1) are gratefully acknowledged. We also thank Heike Hall (Zürich) for her support preparing the hydrogels.

REFERENCES

1. U. Bonse and F. Busch, "X-ray computed microtomography (μCT) using synchrotron radiation (SR)," Prog. Biophys. molec. Biol. **65** (1/2), pp. 133-169, 1996.
2. F. Beckmann, U. Bonse, and T. Biermann, "New developments in attenuation and phase-contrast microtomography using synchrotron radiation with low and high photon energies," Proc. SPIE **3772**, pp. 179-187, 1999.
3. N.J. Schneiders and S.C. Bushong, "Single-step calculation of the MTF from ERF," Medical Physics **5** (1), pp. 31-33, 1978.
4. N.J. Schneiders and S.C. Bushong, "Computer assisted MTF determination in CT," Medical Physics **7** (1), pp. 76-78 1980.
5. K.-L. Eckert, M. Mathey, J. Mayer et al., "Preparation and in vivo testing of porous alumina ceramics for cell carrier applications," Biomaterials **21**, pp. 63-69, 1999.
6. B. Müller, P. Thurner, F. Beckmann et al., "Non-Destructive 3-D Evaluation of Biocompatible Materials by Computed μ-Tomography using Synchrotron Radiation," 6th World Biomaterials Congress, Hawai, U.S.A., 2000.
7. K. Ruloff and F. Widmer, Patent 2117, Switzerland, 1997.
8. K. Ruloff, PhD-Thesis No. 13 893, ETH Zürich, Switzerland, 2000.
9. E. Karamuk, PhD-Thesis No. 14257, 'Embroidered Textiles for Medical Applications', ETH Zürich, 2001.
10. P. Thurner, E. Karamuk, and B. Müller, "3-D characterization of fibroblast cultures on PET textiles," European Cells and Materials **2** (1), pp.57-58, 2001.
11. T. Weitkamp, C. Raven, and A. Snigirev, "An imaging and microtomography facility at the ESRF beamline ID 22," Proc. SPIE **3772**, pp. 311-317, 1999.
12. M.A. Riner, PhD-Thesis No. 13 695, ETH Zürich, Switzerland, 2000.
13. J. Brandt and W. Hein, "Polymer materials in joint surgery," in *Deformation and fracture behavior of polymers*, edited by W. Grellmann and S. Seidler (Springer-Verlag, Berlin New York Heidelberg, 2001), pp. 441-450.
14. D.M. Brunette, P. Tengvall, M. Textor et al., "Titanium in Medicine," in *Enginerering Materials* (Springer, 2001).
15. J. Becker et al., Z. Zahnärtzl. Implantol. **7**, pp. 162-, 1991.
16. P. Thurner, P. Wyss, R. Bernhardt et al., "3-D mikrotomografische (μCT) Untersuchungen der Grenzfläche Knochen/Titan-Implantat," presented at the Gemeinsame Jahrestagung der deutschen Gesellschaft für Biomaterialien und der Chirurgischen Arbeitsgemeinschaft für Biomaterialien der Deutschen Gesellschaft für Chirurgie ‚Biomaterialien im Gelenkbereich', Ulm, Germany, 2000.
17. R. Bernhardt, P. Thurner, D. Scharnweber et al., "Morphological Investigation of Bone-Formation on Surface modified Ti6Al4V-Implants with Micro Computed Tomography (μCT)," presented at the European Society for Biomaterials, 16th European Conference, London, U.K., 2001.
18. R. Bernhardt et al., to be published.